THE JOURNAL OF PHYSICAL CHEMISTRY B

Article

pubs.acs.org/JPCB

Site-Specific Measurements of Lipid Membrane Interfacial Water Dynamics with Multidimensional Infrared Spectroscopy

Derek G. Osborne, Josef A. Dunbar, Jacob G. Lapping, Aaron M. White, and Kevin J. Kubarych*

Department of Biophysics and Chemistry, University of Michigan, 930 North University Avenue, Ann Arbor, Michigan 48109, United States

Supporting Information

ABSTRACT: One route to accessing site-specific dynamical information available with ultrafast multidimensional infrared spectroscopy is the development of robust and versatile vibrational probes. Here we synthesize and characterize a vibrationally labeled cholesterol derivative, (cholesteryl benzoate) chromium tricarbonyl, to probe model lipid membranes, focusing specifically on the membrane−water interface. Utilizing FTIR and polarized-ATR spectroscopies, we determine the location of the chromium tricarbonyl motif to be situated at the water−membrane interface with an orientation of 46 ± 2° relative to the vector normal to the membrane surface. We test the dynamical sensitivity of the (cholesteryl benzoate) chromium tricarbonyl label with two different nonlinear infrared spectroscopy methods, both of which show that the probe is well-suited to the study of membrane dynamics as well as the dynamics of water at the membrane interface. The metal carbonyl vibrational probe located at the surface of a bicelle exhibits spectral diffusion dynamics induced by membrane hydration water that is roughly three times slower than observed using a nearly identical vibrational probe in bulk water.

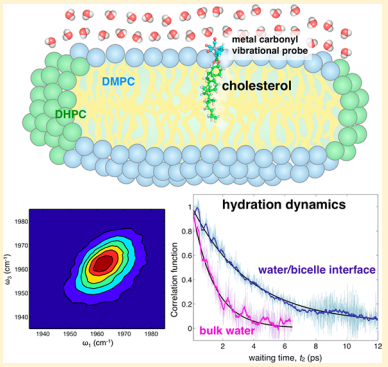

I. INTRODUCTION

The cytoplasm of a living cell is a complex and crowded space containing a diversity of biological macromolecules. Although, in general, no one biological macromolecule is found at a high concentration, macromolecules collectively make up 20−30% of the cytoplasmic volume.[1] The remaining cytoplasmic volume is occupied by water, but because of the ability of extended molecular surfaces to disrupt the hydrogen-bonding network of the interfacial water, relatively little of the cytoplasm's water will exhibit bulk-like properties. Water at the interface of an extended hydrophobic interface is characterized by broken hydrogen bonds[2] creating a layer of constrained water that alters the ultrafast dynamics of water.[3,4] Strongly hydrophilic surfaces also alter water's dynamics by preferentially attracting OH bonds toward the surface while restricting the orientational motion due to the surface's excluded volume.[5] The site specificity of ultrafast vibrational spectroscopy makes it an ideal technique for measuring interfacial water dynamics, although it remains a challenge to access the interfacial water dynamics to the exclusion of the bulk. Recently, we have labeled the interface of hen egg white lysozyme with a covalently bound ruthenium dicarbonyl[6,7] complex and found the dynamics of the interfacial water to be nearly two times slower than that of the bulk.[8] Additionally, we measured the interfacial water dynamics in a series of water−glycerol mixtures and found that despite the viscosity of the bulk increasing by more than two orders of magnitude the dynamics of the interfacial water slowed only three-fold, indicating a weak coupling between the hydration water near the protein and the more distant bulk solution. These measurements on protein surfaces suggest that similar progress might be made by developing sensitive vibrational probes of membranes.

The lipid membrane and its interface with water is central to many chemical reactions critical for life including photosynthesis, ADP phosphorylation, and the initiation of cell signaling cascades.[9] Understanding the dynamical properties of the lipid membrane and its interfacial water is essential to understand biochemical reactions at the lipid membrane.

Ultrafast, multidimensional vibrational spectroscopy can be used to study the dynamics of the lipid membrane's interfacial water, and we demonstrate here the development of novel site specific spectroscopic labels for the lipid membrane.

Despite the ability of 2D-IR to measure interfacial water dynamics, its nonlinear nature requires a vibrational probe to have a strong intrinsic infrared transition strength in an uncluttered region of the spectrum while being highly sensitive of the local environment. In the case of membrane components, there are few natural options, limited largely to the phosphate headgroup of some lipids, which occurs at roughly 1250 cm^{-1}. The phosphate vibration is capable of revealing lipid−water dynamics,[10] but it is clearly not a background-free region of the infrared spectrum. Unlike the case of proteins or nucleobases, there are no strong carbonyl modes that can be accessed to probe lipid membranes. The O−H stretch of water in D_2O has been used to measure the

Special Issue: Michael D. Fayer Festschrift

Received: May 20, 2013
Revised: August 8, 2013
Published: August 9, 2013

dynamics of lipid membrane interfacial water.[10−14] These experiments studied the confined water in reverse micelles, finding the dynamics of interfacial water to be highly micelle size dependent. As the micelles are made smaller, the O−H spectral and reorientational dynamics are found to transition from a mixture of bulk and constrained water at large sizes to primarily constrained interfacial water at smaller sizes.[11,15]

One potential motif is the metal carbonyl organometallic complex that has played a pivotal role in the development of 2DIR experiments used to study intramolecular vibrational energy redistribution,[16,17] chemical exchange,[18,19] energy relaxation,[17] and spectral diffusion.[20,21] In biology, metal carbonyls have found many uses including: carbon-monoxide-releasing molecules (CORM) that release physiological levels of carbon monoxide either spontaneously or upon photo-excitation,[22−24] the Fe-CO motif that is commonly used to probe the hemoglobin and myoglobin active sites,[25−28] a derivative of 17β-etradiol that is capable of measuring hormone receptor concentration,[29,30] and a rhenium tricarbonyl complex that was shown to image the Golgi apparatus of breast cancer cells.[31,32] Recently, a cysteine residue was labeled with a rhenium tricarbonyl,[33] and using 2DIR a surface-bound metal carbonyl complex has successfully measured protein flexibility and the hydration dynamics of globular proteins;[7,8] additional labels should enable us to probe a more diverse range of biological systems.

We propose a novel label to probe the lipid membrane−water interface, (cholesteryl benzoate) chromium tricarbonyl (denoted chol-BCT) based on the benzene chromium tricarbonyl (BCT) piano stool complex (Figure 1). Here we

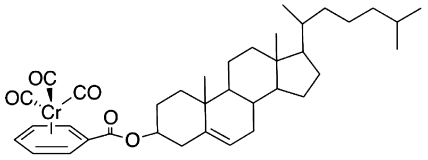

Figure 1. (Cholesteryl benzoate) chromium tricarbonyl (chol-BCT) is synthesized using the hydroxyl group of cholesterol as a nucleophile in a Steglich esterification.

establish a simple protocol to synthesize chol-BCT and embed it in a lipid membrane, characterize the chol-BCT complex, and then using FTIR and polarized-ATR measurements determine the location and relative orientation of chol-BCT once embedded in the lipid bilayer. To demonstrate the robustness of the chol-BCT label, we label both a small unilamellar vesicle (SUV),[34,35] a spherical lipid bilayer with both an external and enclosed aqueous region, as well as a bicelle[36,37] that is a planar bilayer disk composed of a lipid forming the edges of the bicelle and another lipid forming the bilayer. These experiments demonstrate that chol-BCT is a useful probe of both lipid environments. Using 2DIR and a similar four-wave mixing experiment, rapidly acquired spectral diffusion (RASD),[38] we test the ability of chol-BCT to probe water at the interface of a lipid membrane in these experiments and find chol-BCT to be an excellent probe for ultrafast dynamical studies. Lastly, using RASD, we compare the measured dynamics of interfacial water, confirming similar measurements at the protein interface, where hydration water is slowed but only modestly relative to the bulk liquid.

II. EXPERIMENTAL METHODS

Materials. (Ethyl benzoate) chromium tricarbonyl was purchased from Sigma Aldrich and was used without further purification. 1-Palmitoyl-2-oleoyl-*sn*-glycero-3-phosphocholine (POPC), 1-palmitoyl-2-oleoyl-*sn*-glycero-3-phosphoglycerol (POPG), 1,2-dimyristoyl-*sn*-glycero-3-phosphocholine (DMPC), and 1,2-dihexanoyl-*sn*-glycero-3-phosphocholine (DHPC) suspended in chloroform were purchased from Avanti Lipids and used without further purification.

Bicelle Preparation. The DMPC/DHPC/chol-BCT molar ratio was 65:24:1. Lipids and chol-BCT label were cosolublized in chloroform. The chloroform was subsequently removed by evaporation and was then placed under vacuum for 2 h. The mixture was solubilized with a phosphate buffer at pH 7.2 to give a final lipid concentration of 120 mM. Bicelles were formed by a series of five freeze (−78 °C) thaw (30 °C) cycles.

SUV Preparation. Two SUV preparation protocols were used. For the polarized FTIR experiments, the POPC/POPG/chol-BCT molar ratio was 8.2:2.7:1. The mixture was cosolublized in chloroform, dried, and resolubilized with a phosphate buffer at pH 7.2 as previously described to give a final lipid concentration of 25 mM. After a 1 h sonication of the mixture, a clear suspension of SUVs was obtained. The above protocol was also used to produce a sample where choline is the only lipid headgroup to adequately compare the bicelle and SUV samples (Figure 5). The POPC/chol-BCT molar ratio used in these mixtures was 10:1.

Polarized-ATR. Polarized attenuated total reflectance (ATR) spectroscopy was used to measure the orientation of the probe relative to the lipid surface. Polarized-ATR spectroscopy measurements were made with a Jasco FT/IR-4100 spectrometer with a ZnSe 10 internal reflections crystal (Pike Technologies) accessory. The SUVs containing the chol-BCT probe were prepared as described above and were allowed to deposit on the crystal surface for 2 h. Once the SUV is deposited onto the ATR plate, we measure the amplitude of the s and p polarizations separately to determine the order parameter of the transition dipole moment:[39]

$$S_\theta = \frac{(E_x^2 - R^{\mathrm{ATR}}E_y^2 + E_z^2)}{E_x^2 - R^{\mathrm{ATR}}E_y^2 + 2E_z^2} \quad (1)$$

where E_x, E_y, and E_z are the amplitudes of the evanescent waves at the surface of the ATR plate and R_{ATR} is the ratio of the s and p amplitudes, $R_{\mathrm{ATR}} = A_p/A_s$). The order parameter is related to the orientation of the transition dipole moment through:

$$S_\theta = \frac{(3\langle\cos^2\theta\rangle - 1)}{2} \quad (2)$$

where θ is the angle between the transition dipole moment and the vector normal to the surface of the ATR crystal and the brackets indicate the orientational ensemble average.

Four-Wave Mixing Experiments. The experimental setups of 2D infrared spectroscopy (2DIR)[40−42] and RASD[38] used to probe the membrane−water interface with chol-BCT as an ultrafast dynamical probe are described elsewhere. RASD enables rapid experimental determination of the frequency−frequency correlation function (FFCF), $C(t) = <\delta\omega(0)\delta\omega(t)>$, where $\delta\omega(t)$ is the instantaneous frequency fluctuation from the average at time t. The angled brackets indicate an ensemble average. The FFCF is a dynamical quantity that relates to the fluctuations induced by the bath on the spectroscopically

dx.doi.org/10.1021/jp4049428 | J. Phys. Chem. B 2013, 117, 15407−15414

probed degrees of freedom. For metal carbonyl complexes, the primary aspects of water's dynamics that contribute to dynamical frequency modulations are orientational fluctuations,[6−8] which for the case of water occur largely by extended, large-angle jumps.[3,43] Although the RASD method is described in detail in ref 38, because it is new, we briefly summarize the approach here. RASD is a variation on the three-pulse echo peak shift sequence, where, at a fixed coherence time delay, we scan the waiting time delay (t_2) continuously for each of the rephasing ($\mathbf{k}_{sig,reph} = -\mathbf{k}_1 + \mathbf{k}_2 + \mathbf{k}_3$) and nonrephasing ($\mathbf{k}_{sig,reph} = +\mathbf{k}_1 - \mathbf{k}_2 + \mathbf{k}_3$) pulse orderings. By recording the heterodyne detected nonlinear signal and recovering the signal amplitude using spectral interferometry, we are able to construct the inhomogeneity index given by $II = (A_{rephasing} - A_{nonrephasing})/(A_{rephasing} + A_{nonrephasing})$. The inhomogeneity index is proportional to the FFCF.[38,44] The main experimental difference between RASD and three-pulse photon echo peak shift measurements is that RASD does not require the time-consuming scan of the coherence period. Compared with conventional 2D-IR spectroscopy, RASD enables access to the FFCF without the need to record full absorptive 2D spectra at each waiting time.

DFT Calculations. All calculations were performed in Gaussian 09[45] software suite using the B3LYP functional and 6-31+G(d) basis set for all atoms with symmetry disabled. The (ethyl benzoate) chromium tricarbonyl was first minimized before the sodium ion was introduced to the calculations. Geometry was optimized while keeping fixed the sodium-ion-to-chromium-atom distance and was followed by frequency calculations.

Synthesis and Characterization of Metal-Carbonyl-Labeled Cholesterol. Locating chromium tricarbonyl at the water interface of a lipid membrane is achieved by labeling cholesterol with (benzoic acid) chromium tricarbonyl and then embedding the labeled cholesterol within the lipid membrane (Figure 2). The (benzoic acid) chromium tricarbonyl was synthesized with a simple hydrolysis reaction of (ethyl benzoate) chromium tricarbonyl.[46] A mixture of 240 mg of (ethyl benzoate) chromium tricarbonyl and 400 mg of sodium hydroxide in 30 mL of deionized water is stirred in the dark at room temperature for 16 h. The progress of the reaction can be monitored as the orange colored (ethyl benzoate) chromium tricarbonyl is insoluble and the red colored (benzoic acid) chromium tricarbonyl product is soluble. The unreacted (ethyl benzoate) chromium tricarbonyl is removed through ether extraction, the product, (benzoic acid) chromium tricarbonyl, is then precipitated out of solution by acidifying the remaining mixture with hydrochloric acid to pH 2.0, and isolated through a second round of ether extraction.

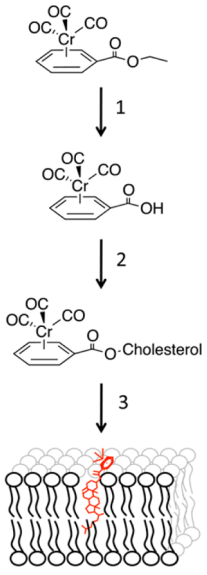

Figure 2. (Ethyl benzoate) chromium tricarbonyl is transformed to the carboxylic acid, to which cholesterol is added by esterification. The labeled cholesterol is readily incorporated into membrane constructs such as bicelles or unilamellar vesicles.

chol-BCT was synthesized using a Steglich esterification.[47] A mixture of 700 mM cholesterol, 30 mM (benzoic acid) chromium tricarbonyl, 4 mM 4-dimethylaminopyradine, and 11 L of *N*,*N*′-diisopropylcarbodiimide in 100 mL of chloroform was placed on ice for 5 min and was then stirred in the dark for 3 h at room temperature. The product was subsequently purified through column chromatography using alumina as the stationary phase and a 3:1 mixture of heptane and ethyl acetate as the mobile phase. The light-yellow chol-BCT is the first product through the column and is isolated from the solvent using a rotary evaporator. The *N*,*N*′-diisopropylcarbodiimide exits the column simultaneously with the chol-BCT; to ensure that the *N*,*N*′-diisopropylcarbodiimide is removed from the sample, we left the product on the rotary evaporator for an additional 20 min after the solvent was removed. The presence of *N*,*N*′-diisopropylcarbodiimide can be assessed by monitoring its C═N═C stretch at 2100 cm^{-1}.

We confirmed the synthesis of chol-BCT with EI+ mass spectroscopy; the molecular ion peaks at 626.3 m/z and 542.3 m/z are of chol-BCT and chol-BCT without the carbonyls, respectively. Further characterization of the product was accomplished using melting point analysis, TGA, and IR. The melting point was measured at 165 °C, whereas the decomposition, measured with thermogravimetric analysis, began at a much higher temperature of ∼290 °C. The IR spectrum of the product − 3097, 2932, 1958, 1881, 1730, 1524, 1499, 1441, 1415, and 1370 cm^{-1} − contains the peaks of both cholesterol and (benzoic acid) chromium tricarbonyl with the exception of the O−H stretch at 3350 cm^{-1} of cholesterol.

III. RESULTS AND DISCUSSION

FTIR Spectroscopy in Solution. To assess the sensitivity of the chromium tricarbonyl motif to the solvent environment, we measure the FTIR spectra of the carbonyl's degenerate asymmetric modes and the symmetric mode, 1928 and 1992 cm^{-1} in hexane, respectively, in multiple solvents with varying polarities (Figure 3). Both the symmetric and asymmetric stretches of BCT are red-shifted with increased polarity, as is observed in many metal carbonyl complexes.[20,48] The symmetric and asymmetric stretches in the most polar solvent examined, dimethyl sulfoxide, are red-shifted 22 and 34 cm^{-1}, respectively, relative to the least polar solvent, hexane. In all measured solvents, the asymmetric peak is broader than the symmetric band, but we do not see noticeable splitting of the degenerate modes in the solvents presented here.

FTIR Spectroscopy in Model Membranes. We assess the location of the chol-BCT carbonyls in an SUV and a bicelle by measuring their FTIR spectrum and comparing them to the spectrum of the chol-BCT in hexane (Figure 4). Because of the high vibrational sensitivity of the chromium tricarbonyl motif, the concentration of chol-BCT in both membrane samples is

dx.doi.org/10.1021/jp4049428 | J. Phys. Chem. B 2013, 117, 15407−15414

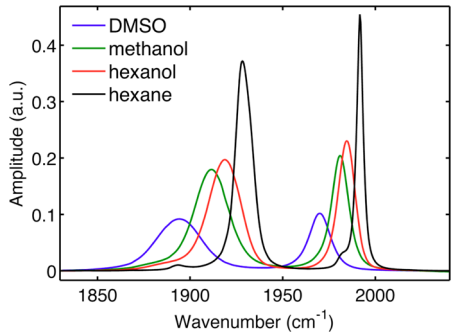

Figure 3. FTIR spectra of the asymmetric and symmetric modes of (benzyl) chromium tricarbonyl in a series of solvents. An increase in solvent polarity tends to red shift both asymmetric and symmetric bands.

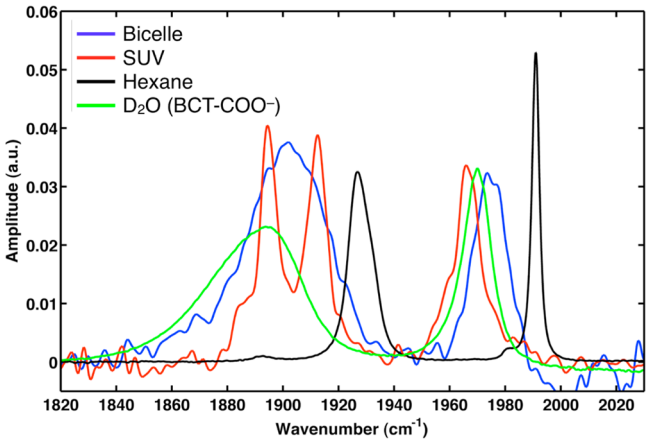

Figure 4. FTIR spectral of chol-BCT in a bicelle and small unilamellar vesicle in water. The spectrum in hexane is also shown as a reference. Chol-BCT in both bilayers is red-shifted relative to the hexane case, indicating that the probe is situated in the more polar headgroup region. The splitting of the asymmetric bands in the SUV suggests that in the SUV the label is situated near an ion. For reference, the spectrum of soluble benzoate chromium tricarbonyl is also shown; the low-frequency bands are broadened but do not exhibit splitting.

<2 mM. The symmetric stretch of chol-BCT in the SUV and the bicelle are red-shifted relative to chol-BCT in hexane by 25 and 17 cm^{-1}, respectively, indicating that the probes in both the SUV and the bicelle are in a highly polar environment. Because lipid bilayers are composed of two regions, the nonpolar alkane chains and the polar head groups at the water interface, the relative red shift of the carbonyls of the chol-BCT probe in the POPC only SUV and the bicelle suggests that the carbonyls are situated near the more polar head groups and the interfacial water. Figure 4 also shows that the degenerate asymmetric stretches in the SUV exhibit distinct splitting that we attribute to the carbonyl's proximity to an ion. We verify the ion's role in splitting the degenerate bands by performing DFT calculations on (ethyl benzoate) chromium tricarbonyl at a fixed distance from a sodium ion. The smaller size of (ethyl benzoate) chromium tricarbonyl allows for shorter computational time relative to that required for chol-BCT, yet it should be an adequate model of chol-BCT. We performed all calculations in vacuum, which enhances the effect of degeneracy splitting; if a solvent were to be introduced, then we would expect the additional atoms to shield the probe from the ion making the distance at which the probe senses the ion and the magnitude of the splitting to be much smaller. When the sodium ion is excluded from the calculation, the ethyl benzoate alone is capable of breaking the symmetry and splits the degenerate band by 7 cm^{-1} (Table 1). The sodium ion located 5 Å from

Table 1. DFT Calculated Vibrational Frequencies of the Three Carbonyl Modes of (Ethyl Benzoate) Chromium Tricarbonyl Alone, and with a Sodium Ion Fixed 5 and 10 Å from the Chromium Atom

charge distance	symmetric frequency (cm^{-1})	asymmetric 1 frequency (cm^{-1})	asymmetric 2 frequency (cm^{-1})	splitting (cm^{-1})
no charge	2057	2005	1998	7
5 Å	2071	2030	1835	195
10 Å	2050	1999	1979	20

the chromium atom splits the band by 195 cm^{-1}, while a 10 Å distance results in a 20 cm^{-1} splitting. Hence, the pronounced splitting appears to be indicative of local electrostatics due to charges associated with the membrane, but in a real solution the solvent will shield local charges to some extent. Additionally, previous experimental work found that a contact ion pair does not induce a splitting of a degenerate asymmetric mode.[49] For comparison, we also show benzoate chromium tricarbonyl in D_2O, where the band positions are similar to those in the labeled cholesterol, but there is no observable splitting of the low-frequency bands. The spectrum in water strongly resembles that of chol-BCT in bicelles.

The fact that the SUV-bound label exhibits pronounced splitting whereas bicelle-bound label does not suggests that the labels are in different environments in the two cases. The oleoyl and palmitoyl alkane chains of the POPC SUV are longer and less saturated, 18:1 and 16:0, respectively, than the myristoyl alkane chains, 14:0, of DMPC and the heptanoyl alkane chains, 7:0, of DHPC used in the bicelles. Although the shape of the SUV is spherical while the bicelle is planar, the splitting remains when the SUV is deposited on a planar surface (Figure 5); therefore, the curvature of the SUV is likely not the origin of the degeneracy splitting. Thus, we propose that the lack of splitting in the bicelle is due to its shorter and saturated alkane chains pushing the carbonyls of chol-BCT further into the aqueous solvent, reducing their proximity to the charged head groups. Future work will investigate the lipid chain-length dependences of the linear spectra and the ultrafast dynamics probed with nonlinear spectroscopy.

Polarized-ATR. Although the FTIR experimental data gives information on the location of the carbonyls in the membranes, it does not give information on the relative orientation of the carbonyls; this information is determined using polarized-ATR (Figure 5). We measure the p and s polarization amplitudes of the symmetric mode, and with eqs 1 and 2 we determine the orientation of the transition dipole moment of the symmetric mode relative to the ATR crystal surface. Because the lipid bilayer is deposited onto the surface of the ATR trough and the transition dipole moment of the symmetric stretch is perpendicular to the benzyl ring, measuring the ratio of the s and p polarization amplitudes of the symmetric stretch is a measure of the orientation of the of the benzyl ring relative to the lipid membrane.[39] We measure the ratio of p and s amplitudes, A_p/A_s, to be 2.5, indicating the vector perpendicular to the benzyl ring makes an angle of 46 ± 2° relative to the vector normal to the membrane surface (Figure 5B). The structure of the chol-BCT probe is flexible about the ester

dx.doi.org/10.1021/jp4049428 | J. Phys. Chem. B 2013, 117, 15407−15414

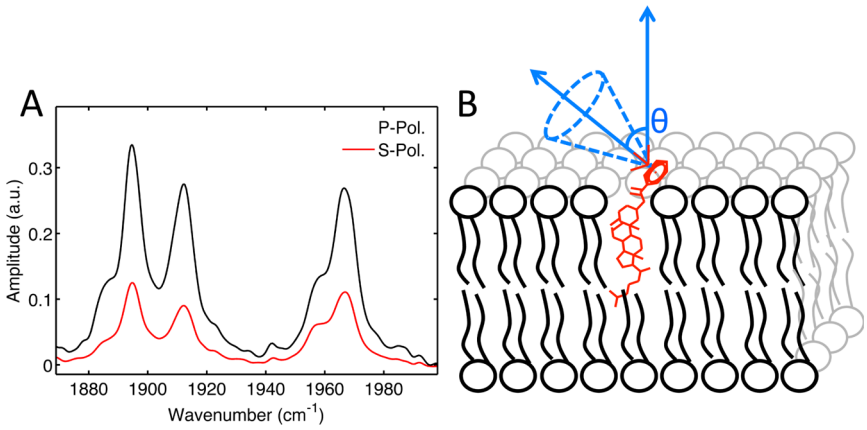

Figure 5. Polarized ATR-FTIR spectra showing the relative s- and p-polarized amplitudes of the symmetric stretch (A) to determine the relative orientation of the carbonyls. These measurements suggest that the vector perpendicular to the benzene ring is at an angle of 46 ± 2° from the vector normal to the membrane surface.

bond, allowing for a distribution of probe orientations that gives an average angle of 46 ± 2°. This method of orientation determination does not permit an estimate of the cone angle.

2DIR Spectroscopy in Bicelles. We test the capability of chol-BCT to serve as a dynamical probe of the membrane−water interface by analyzing two different four-wave mixing experiments on the symmetric stretch in a bicelle at 1973 cm^{-1}. The 2DIR spectrum is noticeably elongated along the $\omega_1 = \omega_3$ diagonal, indicating that the band is inhomogeneously broadened due to a distribution of local environments and is capable of measuring the microenvironment dynamics near the tricarbonyls of chol-BCT (Figure 6). Such an inhomogeneous broadening is expected based on the broad, ∼25 cm^{-1}, widths measured in the 1-D FTIR spectra (Figure 4).

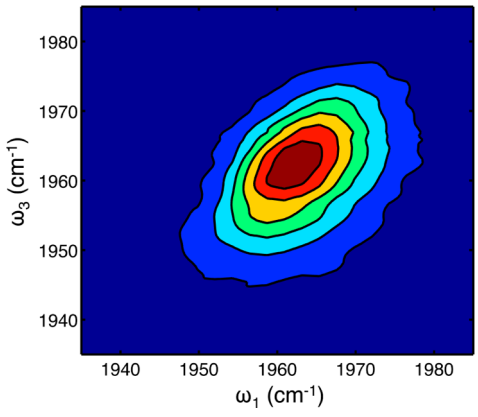

Figure 6. 2DIR rephasing spectrum of chol-BCT embedded in a bicelle recorded at a waiting time of 250 fs. Diagonal elongation is characteristic of inhomogeneous broadening. Signal levels are sufficient to permit 2DIR studies on dilute samples.

Rapidly Acquired Spectral Diffusion. We test the ability of chol-BCT to measure the interfacial water dynamics by measuring the frequency−frequency correlation function (FFCF) of chol-BCT with RASD. Additionally, to understand how the interfacial water dynamics are constrained relative to the bulk, we measure the FFCF of the chromium tricarbonyl motif in bulk water. Because chol-BCT is insoluble, we use (benzoate) chromium tricarbonyl in the bulk water measurements (Figure 7A). Fitting the FFCF of the bulk D_2O measurement to an exponential yields a 1.4 ± 0.1 ps time constant, which agrees with our previous studies of small metal carbonyl complexes in D_2O.[8] In the bicelle case, we fit the data to an exponential with a 3.5 ± 0.2 ps time constant and a slight offset of 0.04. A biexponential fit to the rephasing data (Figure 7B) yields a major decay component with a time constant of 3.30 ± 0.14 ps (70% of the signal amplitude) and a minor component (30% of the signal amplitude) of 1.05 ± 0.23 ps. We attribute the faster time constant to intramolecular vibrational redistribution and the slower time constant to the vibrational lifetime. Given the very rapid vibrational relaxation, we can confirm that the carbonyl probes are exposed to water.[6−8] The 1.4 ps spectral diffusion time constant of bulk water is similar to that measured using 2DIR spectroscopy of the OH stretch in D_2O,[50] suggesting that the chromium tricarbonyl is a direct measure of the hydrogen bond network reorganization while reinforcing the picture that small molecular solutes exert only negligible influence on the dynamics of hydration water. We note, however, that very small solutes, such as F^- or divalent cations (Mg^{2+}, Ca^{2+}, etc.), can significantly distort the structure and dynamics of the water in the first solvation shell.[4,51,52] The time scale sensed by the interfacial label is similar in magnitude to that of a metal carbonyl probe at the surface of lysozyme,[8] which supports the general conclusion that extended biological interfaces place dynamical constraints on the hydration water but that the slowdown is modest. Our previous work, which quantitatively agreed with explicit solvent molecular dynamics simulations by Laage et al., found the slowdown to be a factor of two relative to the bulk liquid. Here, where the surface is likely to be even flatter than the protein and rich in ions, we observe a similar slowdown of a factor of two to three. Our measurements are consistent with experiments on hydrated DNA, where slowdown factors of two to three have been reported.[53,54] Our finding of a modest slowdown is also consistent with simulation results on model surfaces with arbitrarily tunable hydrophobicity.[5] Hence, our data indicate that as with proteins the orientational dynamics of water at the membrane interface are disrupted by the lack of available three-body partners required for the extended jump mechanism of water hydrogen switching. Future studies will investigate the influence of macromolecular crowding on the hydration water dynamics, where recent NMR experiments have shown relatively weak coupling between the

dx.doi.org/10.1021/jp4049428 | J. Phys. Chem. B 2013, 117, 15407−15414

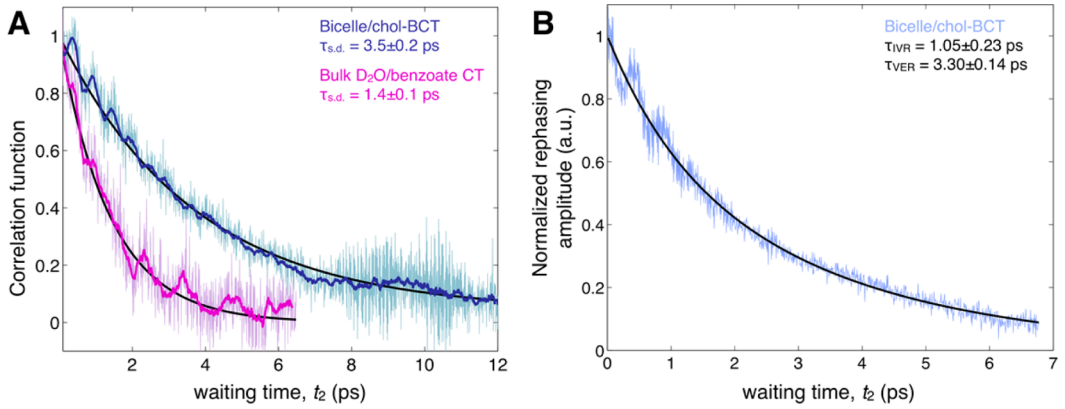

Figure 7. (A) Rapidly acquired spectral diffusion (RASD) measures the FFCF of the chromium tricarbonyl motif in bulk water and at the bicelle–water interface. As we have found in several other examples,[5] the small-molecule probe reports bulk water dynamics in agreement with direct 2D-IR measurements of HOD/D_2O. The interfacial water as sensed by the probe exhibits two to three times slower spectral dynamics than bulk water due to constraints imposed by the interface. The faint lines are the full data set; the thick colored lines are the result of a 100 fs windowed moving average. The fits are shown as black lines. (B) Rephasing decay for the bicelle sample showing the full data set (blue) and the biexponential fit. The sub-5-ps lifetime is indicative of water exposure.

hydration shell water and the bulk solution,[55] similar to our previous work on protein–hydration coupling.

IV. CONCLUSIONS

We have implemented a novel ultrafast vibrational label to probe model biological membranes, focusing specifically on the membrane's interface with its hydrating water. The strong intrinsic infrared transition strength and high degree of sensitivity to its local environment of chol-BCT suggests that chol-BCT is a promising probe of the membrane–water interface. Here we have developed a protocol for placing the chromium tricarbonyl motif at the interface of water and the lipid membrane by first synthesizing chol-BCT and then embedding the chol-BCT label in the lipid membrane. We characterized the chol-BCT label with mass spectrometry, FTIR spectroscopy, melting point, and thermogravimetric analysis and determined the location and orientation of the chromium tricarbonyl relative to the lipid membrane through FTIR and polarized-ATR spectroscopies. These experiments suggest that the chromium tricarbonyl motif is positioned at the membrane–water interface and is capable of measuring the dynamics of interfacial water. The measurements of chol-BCT with nonlinear infrared experiments 2D-IR and RASD suggest that chol-BCT is a useful label of interfacial dynamics. Comparing the FFCF time scales of the bulk and the interfacial measurements, the interfacial water exhibits a nearly three-fold slowdown relative to the bulk, suggesting that the interfacial water is indeed constrained. We have also used the synthesis protocol presented here to label multiple hydroxyl groups not included in this manuscript including glyceryl 1,3-dipamitate, POPG, and *n*-butanol, suggesting that this protocol can be used in diverse settings. Potentially, with the use of other similar piano stool metal carbonyl complexes (e.g., cyclopentadienyl manganese tricarbonyl), multiple chemical groups of a lipid bilayer can be labeled with the different metal carbonyl complexes, allowing for additional experiments including bilayer aggregation, where different probes can observe distinct components in parallel.

■ ASSOCIATED CONTENT

Supporting Information

The complete ref 45 is given. This material is available free of charge via the Internet at http://pubs.acs.org.

■ AUTHOR INFORMATION

Corresponding Author

*E-mail: kubarych@umich.edu.

Notes

The authors declare no competing financial interest.

■ ACKNOWLEDGMENTS

This work was supporting by the National Science Foundation (CHE-0748501) and the Camille & Henry Dreyfus Foundation.

■ REFERENCES

(1) Zimmerman, S. B.; Trach, S. O. Estimation of Macromolecule Concentrations and Excluded Volume Effects for the Cytoplasm of Escherichia-Coli. *J. Mol. Biol.* **1991**, *222*, 599–620.
(2) Chandler, D. Interfaces and the Driving Force of Hydrophobic Assembly. *Nature* **2005**, *437*, 640–647.
(3) Laage, D.; Hynes, J. T. A Molecular Jump Mechanism of Water Reorientation. *Science* **2006**, *311*, 832–835.
(4) Laage, D.; Hynes, J. T. Reorientional Dynamics of Water Molecules in Anionic Hydration Shells. *Proc. Natl. Acad. Sci. U.S.A.* **2007**, *104*, 11167–11172.
(5) Stirnemann, G.; Castrillon, S. R-V.; Hynes, J. T.; Rossky, P. J.; Debenedetti, P. G.; Laage, D. Non-Monotonic Dependence of Water Reorientation Dynamics on Surface Hydrophilicity: Competing Effects of the Hydration Structure and Hydrogen-Bond Strength. *Phys. Chem. Chem. Phys.* **2011**, *13*, 19911–19917.
(6) King, J. T.; Ross, M. R.; Kubarych, K. J. Water-Assisted Vibrational Relaxation of a Metal Carbonyl Complex Studied with Ultrafast 2D-IR. *J. Phys. Chem. B* **2012**, *116*, 3754–3759.
(7) King, J. T.; Arthur, E. J.; Brooks, C. L.; Kubarych, K. J. Site-Specific Hydration Dynamics of Globular Proteins and the Role of Constrained Water in Solvent Exchange with Amphiphilic Cosolvents. *J. Phys. Chem. B* **2012**, *116*, 5604–5611.
(8) King, J. T.; Kubarych, K. J. Site-Specific Coupling of Hydration Water and Protein Flexibility Studied in Solution with Ultrafast 2D-IR Spectroscopy. *J. Am. Chem. Soc.* **2012**, *134*, 18705–18712.

(9) Nelson, D. L.; Cox, M. M. *Principles of Biohemistry*, 5th ed.; W. H. Freeman and Company: New York, 2008.
(10) Costard, R.; Levinger, N. E.; Nibbering, E. T. J.; Elsaesser, T. Ultrafast Vibrational Dynamics of Water Confined in Phospholipid Reverse Micelles. *J. Phys. Chem. B* **2012**, *116*, 5752−5759.
(11) Fenn, E. E.; Wong, D. B.; Fayer, M. D. Water Dynamics in Small Reverse Micelles in Two Solvents: Two-Dimensional Infrared Vibrational Echoes with Two-Dimensional Background Subtraction. *J. Chem. Phys.* **2011**, *134*, 054512.
(12) Fenn, E. E.; Wong, D. B.; Giammanco, C. H.; Fayer, M. D. Dynamics of Water at the Interface in Reverse Micelles: Measurements of Spectral Diffusion with Two-Dimensional Infrared Vibrational Echoes. *J. Phys. Chem. B* **2011**, *115*, 11658−11670.
(13) Levinger, N. E.; Costard, R.; Nibbering, E. T. J.; Elsaesser, T. Ultrafast Energy Migration Pathways in Self-Assembled Phospholipids Interacting with Confined Water. *J. Phys. Chem. A* **2011**, *115*, 11952−11959.
(14) Moilanen, D. E.; Fenn, E. E.; Wong, D.; Fayer, M. D. Water Dynamics at the Interface in AOT Reverse Micelles. *J. Phys. Chem. B* **2009**, *113*, 8560−8568.
(15) Fayer, M. D. Dynamics of Water Interacting with Interfaces, Molecules, and Ions. *Acc. Chem. Res.* **2012**, *45*, 3−14.
(16) King, J. T.; Anna, J. M.; Kubarych, K. J. Solvent-hindered Intramolecular Vibrational Redistribution. *Phys. Chem. Chem. Phys.* **2011**, *13*, 5579−5583.
(17) Khalil, M.; Demirdoven, N.; Tokmakoff, A. Coherent 2D IR Spectroscopy: Molecular Structure and Dynamics in Solution. *J. Phys. Chem. A* **2003**, *107*, 5258−5279.
(18) Anna, J. M.; Kubarych, K. J. Watching Solvent Friction Impede Ultrafast Barrier Crossings: A Direct Test of Kramers Theory. *J. Chem. Phys.* **2010**, *133*, 174506.
(19) Cahoon, J. F.; Sawyer, K. R.; Schlegel, J. P.; Harris, C. B. Determining Transition-State Geometries in Liquids using 2D-IR. *Science* **2008**, *319*, 1820−1823.
(20) King, J. T.; Baiz, C. R.; Kubarych, K. J. Solvent-Dependent Spectral Diffusion in a Hydrogen Bonded "Vibrational Aggregate". *J. Phys. Chem. A* **2010**, *114*, 10590−10604.
(21) King, J. T.; Ross, M. R.; Kubarych, K. J. Ultrafast alpha-Like Relaxation of a Fragile Glass-Forming Liquid Measured Using Two-Dimensional Infrared Spectroscopy. *Phys. Rev. Lett.* **2012**, *108*, 157401.
(22) Clark, J. E.; Naughton, P.; Shurey, S.; Green, C. J.; Johnson, T. R.; Mann, B. E.; Foresti, R.; Motterlini, R. Cardioprotective Actions by a Water-Soluble Carbon Monoxide-Releasing Molecule. *Circ. Res.* **2003**, *93*, E2−E8.
(23) Foresti, R.; Hammad, J.; Clark, J. E.; Johnson, T. R.; Mann, B. E.; Friebe, A.; Green, C. J.; Motterlini, R. Vasoactive Properties of CORM-3, a Novel Water-soluble Carbon Monoxide-releasing Molecule. *Br. J. Pharmacol.* **2004**, *142*, 453−460.
(24) Sawle, P.; Foresti, R.; Mann, B. E.; Johnson, T. R.; Green, C. J.; Motterlini, R. Carbon Monoxide-Releasing Molecules (CO-RMs) Attenuate the Inflammatory Response Elicited by Lipopolysaccharide In RAW264.7 Murine Macrophages. *Br. J. Pharmacol.* **2005**, *145*, 800−810.
(25) Caughey, W. S.; Shimada, H.; Choc, M. G.; Tucker, M. P. Dynamic Protein Structures - Infrared Evidence for 4 Discrete Rapidly Interconverting Conformers at The Carbon-Monoxide Binding-Site of Bovine Heart Myoglobin. *Proc. Natl. Acad. Sci. U.S.A.* **1981**, *78*, 2903−2907.
(26) Lim, M. H.; Jackson, T. A.; Anfinrud, P. A. Ultrafast Rotation and Trapping of Carbon Monoxide Dissociated from Myoglobin. *Nat. Struct. Biol.* **1997**, *4*, 209−214.
(27) Tsubaki, M.; Srivastava, R. B.; Yu, N. T. Resonance Raman Investigation of Carbon-Monoxide Bonding in (Carbon Monoxy) Hemoglobin and (Carbon Monoxy) Myoglobin - Detection of Fe-CO Stretching nd Fe-CO Bending Vibrations and Influence of the Quaternary Structure Change. *Biochemistry* **1982**, *21*, 1132−1140.
(28) Alben, J. O.; Caughey, W. S. AN Infrared Study of Bound Carbon Monoxide in Human Red Blood Cell Isolated Hemoglobin and Heme Carbonyls. *Biochemistry* **1968**, *7*, 175−183.
(29) Jaouen, G.; Vessieres, A.; Top, S.; Ismail, A. A.; Butler, I. S. Metal-Carbonyl Fragments as a New Class of Markers in Molecular Biology. *J. Am. Chem. Soc.* **1985**, *107*, 4778−4780.
(30) Top, S.; Jaouen, G.; Vessieres, A.; Abjean, J. P.; Davoust, D.; Rodger, C. A.; Sayer, B. G.; McGlinchey, M. J. Chromium Tricarbonyl Complexes of Estradiol Derivatives - Differentiation of Alpha-Diastereoisomer and Beta-Diastereoisomers Using One-Dimensional and Two-Dimensional NMR Spectroscopy at 500 MHz. *Organometallics* **1985**, *4*, 2143−2150.
(31) Clede, S.; Lambert, F.; Sandt, C.; Gueroui, Z.; Refregiers, M.; Plamont, M.-A.; Dumas, P.; Vessieres, A.; Policar, C. A Rhenium Tris-Carbonyl Derivative as a Single Core Multimodal Probe for Imaging (SCoMPI) Combining Infrared and Luminescent Properties. *Chem. Commun.* **2012**, *48*, 7729−7731.
(32) Policar, C.; Waern, J. B.; Plamont, M.-A.; Clede, S.; Mayet, C.; Prazeres, R.; Ortega, J.-M.; Vessieres, A.; Dazzi, A. Subcellular IR Imaging of a Metal-Carbonyl Moiety Using Photothermally Induced Resonance. *Angew. Chem., Int. Ed.* **2011**, *50*, 860−864.
(33) Woys, A. M.; Mukherjee, S. S.; Skoff, D. R.; Moran, S. D.; Zanni, M. T. A Strongly Absorbing Class of Non-Natural Labels for Probing Protein Electrostatics and Solvation with FTIR and 2D IR Spectroscopies. *J. Phys. Chem. B* **2013**, *117*, 5009−5018.
(34) Pitcher, W. H.; Huestis, W. H. Preparation and Analysis of Small Unilamellar Phospholipid Vesicles of a Uniform Size. *Biochem. Biophys. Res. Commun.* **2002**, *296*, 1352−1355.
(35) Szoka, F. C.; Milholland, D.; Barza, M. Effect of Lipid-Composition and Liposome Size on Toxicity and Invitro Fungicidal Activity of Liposome-Intercalated Amphotericin-B. *Antimicrob. Agents Chemother.* **1987**, *31*, 421−429.
(36) Sanders, C. R.; Prosser, R. S. Bicelles: A Model Membrane System for All Seasons? *Structure* **1998**, *6*, 1227−1234.
(37) Vold, R. R.; Prosser, R. S.; Deese, A. J. Isotropic Solutions of Phospholipid Bicelles: A New Membrane Mimetic for High-Resolution NMR Studies of Polypeptides. *J. Biomol. NMR* **1997**, *9*, 329−335.
(38) Osborne, D. G.; Kubarych, K. J. Rapid and Accurate Measurement of the Frequency-Frequency Correlation Function. *J. Phys. Chem. A* **2013**, *117*, 5891−5898.
(39) Tamm, L. K.; Tatulian, S. A. Infrared Spectroscopy of Proteins and Peptides in Lipid Bilayers. *Q. Rev. Biophys.* **1997**, *30*, 365−429.
(40) Nee, M. J.; Baiz, C. R.; Anna, J. M.; McCanne, R.; Kubarych, K. J. Multilevel Vibrational Coherence Transfer and Wavepacket Dynamics Probed with Multidimensional IR Spectroscopy. *J. Chem. Phys.* **2008**, *129*, 084503.
(41) Anna, J. M.; Nee, M. J.; Baiz, C. R.; McCanne, R.; Kubarych, K. J. Measuring Absorptive Two-Dimensional Infrared Spectra Using Chirped-Pulse Upconversion Detection. *J. Opt. Soc. Am. B* **2010**, *27*, 382−393.
(42) Nee, M. J.; McCanne, R.; Kubarych, K. J.; Joffre, M. Two-Dimensional Infrared Spectroscopy Detected by Chirped Pulse Upconversion. *Opt. Lett.* **2007**, *32*, 713−715.
(43) Sterpone, F.; Stirnemann, G.; Laage, D. Magnitude and Molecular Origin of Water Slowdown Next to a Protein. *J. Am. Chem. Soc.* **2012**, *134*, 4116−4119.
(44) Roberts, S. T.; Loparo, J. J.; Tokmakoff, A. Characterization of Spectral Diffusion from Two-Dimensional Line Shapes. *J. Chem. Phys.* **2006**, *125*, 084502.
(45) Frisch, M. J.; Trucks, G. W.; Schlegel, H. B.; Scuseria, G. E.; Robb, M. A.; Cheeseman, J. R.; Scalmani, G.; Barone, V.; Mennucci, B.; Petersson, G. A., et al. *Gaussian 09*, A.02; Gaussian, Inc.: Wallingford, CT, 2009.
(46) Nicholls, B.; Whiting, M. C. The Organic Chemistry of the Transition Elements 0.1. Tricarbonylchromium Derivatives of Aromatic Compounds. *J. Chem. Soc.* **1959**, 551−556.
(47) Neises, B.; Steglich, W. 4-Dialkylaminopyridines as Acylation Catalysts 0.5. Simple Method for Esterification of Carboxylic Acids. *Angew. Chem., Int. Ed.* **1978**, *17*, 522−524.

(48) Creaser, C. S.; Fey, M. A.; Stephenson, G. R. Environment Sensitivity of IR-Active Metal-Carbonyl Probe Groups. *Spectrochim. Acta, Part A* **1994**, *50*, 1295−1299.
(49) Anson, C. E.; Creaser, C. S.; Stephenson, G. R. [(η^6-Benzocrown Ether)$Cr(CO)_3$] Complexes as FTIR-Readable Molecular Sensors for Alkali-Metal Cations. *J. Chem. Soc., Chem. Commun.* **1994**, 2175−2176.
(50) Roberts, S. T.; Ramasesha, K.; Tokmakoff, A. Structural Rearrangements in Water Viewed Through Two-Dimensional Infrared Spectroscopy. *Acc. Chem. Res.* **2009**, *42*, 1239−1249.
(51) Boisson, J.; Stirnemann, G.; Laage, D.; Hynes, J. T. Water reorientation dynamics in the first hydration shells of F^- and I^-. *Phys. Chem. Chem. Phys.* **2011**, *13*, 19895−19901.
(52) Laage, D.; Stirnemann, G.; Hynes, J. T. Why Water Reorientation Slows without Iceberg Formation around Hydrophobic Solutes. *J. Phys. Chem. B* **2009**, *113*, 2428−2435.
(53) Szyc, L.; Yang, M.; Nibbering, E. T. J.; Elsaesser, T. Ultrafast Vibrational Dynamics and Local Interactions of Hydrated DNA. *Angew. Chem., Int. Ed.* **2010**, *49*, 3598−3610.
(54) Yang, M.; Szyc, L.; Elsaesser, T. Decelerated Water Dynamics and Vibrational Couplings of Hydrated DNA Mapped by Two-Dimensional Infrared Spectroscopy. *J. Phys. Chem. B* **2011**, *115*, 13093−13100.
(55) Franck, J. M.; Scott, J. A.; Han, S. Nonlinear Scaling of Surface Water Diffusion with Bulk Water Viscosity of Crowded Solutions. *J. Am. Chem. Soc.* **2013**, *135*, 4175−4178.